

DETERMINATION OF Ge PHOTODIODE BASED NEAR INFRARED DETECTION ELEMENT'S OPTICAL RESPONSIVITY

Özcan Bazkır and A. Kamuran Türkoğlu

TUBITAK-UME, Optics Laboratory, Gebze/KOCAELİ, Turkey

Received: December 13, 2009

Abstract. Quantum detectors made from single photodiodes have both polarization dependency and high front surface reflectance losses, which results in low external quantum efficiency and also instability in the responsivity. These effects can be overcome with a special detectors made from combinations of photodiodes on a skeleton in such a configuration trapping the reflected beams. Hence, this work describes both construction of Near Infrared (NIR) optical detection element, made from a skeleton and three large area (10 mm x 10 mm) windowless Germanium (Ge) photodiodes, and also determination of its responsivity scale. The responsivity scale was traced to primary systems at laser wavelengths via improved laser stabilization optics and electrical substitution cryogenic radiometer system. Moreover, it was expanded to other wavelengths in its active range by using physical models developed for the reflectance and quantum efficiency.

1. INTRODUCTION

Responsivity is simply current or voltage response of detectors to incident optical power. Accurate determination of current/voltage, incident optical power and their stabilities are crucially important for the users in the optical metrology and industries like; defense, health, communication, space, ect. In order to meet the expectations coming from these users, new measurement systems and techniques have been developed and used especially in metrology institutions.

For the absolute optical power measurements laser based cryogenic radiometer, which works at liquid helium temperature and compared to standard radiometers has about 1000 times better accuracy, developed by Quinn and Martin at the National Physical Laboratory, UK (NPL) [1] has been used.

In order to transfer the absolute optical power to other measurement systems photodiode based trap

detectors constructed by Zalewski et al. [2] and developed by Fox [3] have been used. The aim in the construction of trap detectors was to remove the polarization sensitivity of detector to incident light and reduce the high reflection losses of photodiodes and thereby increase external quantum efficiency.

Today, the densities of infrared activities in active and passive defense technologies are obvious. Besides this, fiber optic networks in modern communications bring the widespread use of sensitive devices at 850 nm, 1310 nm, and 1550 nm infrared wavelengths. In this and similar sectors, in the radiometry field, in order to improve the efficiency of detection materials, construction and characterization of sensitive, stable and accurate reference devices are subject of current researches. Covering both Nd:YAG laser wavelength and fiber optics communication wavelengths (850 nm, 1310 nm, and 1550 nm) the near infrared region (NIR) is an impor-

Corresponding author: Özcan Bazkır, e-mail: ozcan.bazkir@ume.tubitak.gov.tr

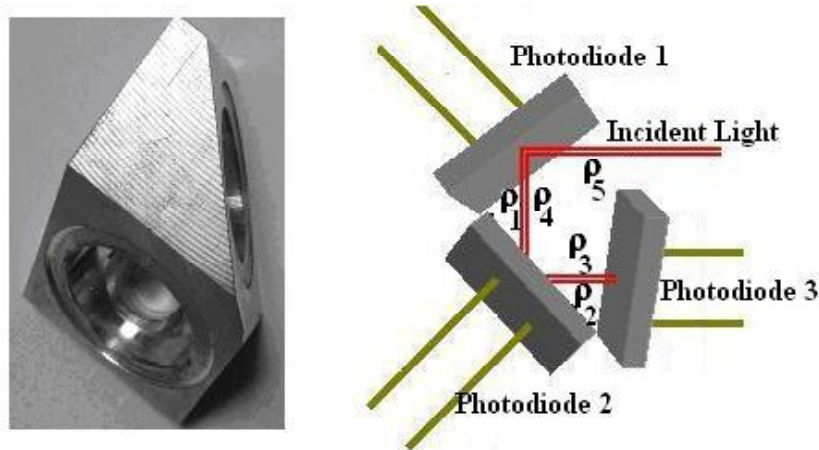


Fig. 1. Geometrical configurations of photodiodes in the reflection type trap detector.

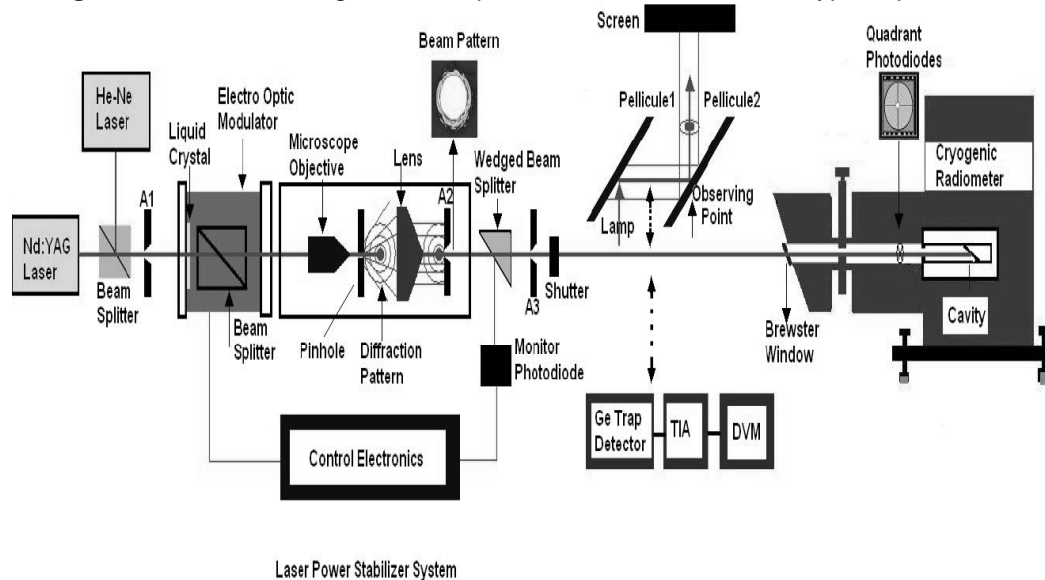


Fig. 2. High accuracy optical power measurement system.

tant region in optical metrology and the construction of sensitive detection element is seriously important.

To construct trap detectors working in the NIR region, InGaAs and Ge photodiodes can be used. Ge photodiodes in some respects have low optical performances (low shunt current, low spatial uniformity...) compared to InGaAs photodiodes [4,5]. However, due to their low prices they have been preferred to be used in the trap detector construction. Moreover, it has been shown that both improvements in the Ge production, which results in good spatial uniformity, low reflectance losses, high quantum efficiency, and measurement conditions such as; low temperature measurements, light beam stabilization reduces the Ge photodiodes drawbacks to desirable level [5].

2. DESIGN AND CONSTRUCTION OF THREE ELEMENT REFLECTION TYPE Ge PHOTODIODE BASED TRAP DETECTOR

A trap detector made from geometrical combinations of several photodiodes in such a way that reflected light from a photodiode can be trapped by other photodiodes and hence most of the incident light can be absorbed within the structure. Depending on the geometrical configuration and number of photodiodes, trap detectors are classified as reflection, transmission and tunnel traps [3,6-8]. In this work, a three element reflection type trap detector was designed in such a way that front surfaces of two photodiodes mounted on its skeleton make an angle of 45° with respect to the incident radiation and that of the third one is just perpendicular to the

incident beam, Fig. 1. Hence, the incident beam undergoes five reflections; two of them make 45° angle with the perpendicular (s) plane of polarization, two make 45° angle with the parallel (p) plane of polarization and one normal incidence. Thus, in this process most of the radiation is being absorbed by photodiodes and the remaining beam returns back along the incoming beam.

The photodiodes used in this structure were decided by considering the trap detector's metrological applications. In order to have high responsivity and large linearity windowless photodiodes having large sensitive area (10 mm x 10 mm) were used. It has been known that the size of sensitive area in photodiodes has an important effect on their optical properties. A large sensitive area although leads to high capacitance, high dark current and high noise equivalent power in a photodiode, it can also enable higher responsivity and large linearity range [9,10].

3. REALIZATION OF RESPONSIVITY SCALE

3.1. Absolute power and responsivity measurements

The absolute responsivity of Ge photodiode based trap detector was measured using high accuracy optical power measurement system, which as shown in Fig. 2 has two parts; laser power stabilizer (LPS) and electrical substitution cryogenic radiometer (ESCR) systems, which is designed to be used with a collimated and vertically polarized light beam having power level ranging from few μW to 1 mW. As radiant source Nd:YAG laser was used, which was aligned to pass through the LPS for the compensation of power fluctuations and generation of desired beam profile having Gaussian distribution. The LPS consists of an electro-optic modulator (EOM), temperature controlled monitor photodiode and control electronics. The laser beam incident on the EOM unit passes through a liquid crystal and polarizing beam splitter respectively. The optical beam leaving from EOM is partially reflected by the wedged beam splitter and directed to incident on the monitor photodiode which convert optical beam to electrical signal. Signal processing unit send this signal back to the EOM for controlling the beam transmittance and getting a constant signal power output. Using this technique the output stability of 2×10^{-4} level was reached. Moreover, the spatial profile of the laser beam was adjusted (3 mm diameter Gaussian beam) using a microscope, pin-hole and lens combinations shown in this system.

The entrance window of the ESCR is made from a fused silica glass which is aligned to Brewster angle. The window was cleaned using suitable solutions and its transmittance was measured as 0.9966 with an uncertainty of 3×10^{-5} before and after the optical power measurements.

To align the Nd: YAG laser beam into the radiometer cavity, Nd: YAG laser beam was superimposed with visible He-Ne laser beam on the beamsplitter. Both laser beams were adjusted to same diameters and their divergences at radiometer cavity point were controlled. He-Ne laser was aligned into the cavity using pellicules and quadrant photodiodes at the radiometer and cavity entrance points respectively.

Optical power measurement of Nd:YAG laser beam was performed using static substitution method. This method is based on sandwiching optical temperature between two electrical temperature points. In the static substitution method, a measurement cycle consists of three optical points and two electrical points calculated to be slightly above and slightly below the optical value [11]. The optical and electrical points are alternate in the order: optical (T_{op1}), electrical low (T_{L1} , P_{L1}), optical (T_{op2}), electrical high (T_{H1} , P_{H1}), optical (T_{op3}) electrical low (T_{L2} , P_{L2}), optical (T_{op4}), electrical high (T_{H2} , P_{H2}). The optical power can be calculated from the following equation [11].

$$P_{op} = \frac{1}{3} \left\{ \left[P_{L1} + \frac{P_{H1} - P_{L1}}{T_{H1} - T_{L1}} \left(\sum_{j=1}^3 \left(\frac{T_{op,j}}{3} \right) - T_{L1} \right) \right] + \left[P_{H1} + \frac{P_{L2} - P_{H1}}{T_{L2} - T_{H1}} \left(\sum_{j=2}^4 \left(\frac{T_{op,j}}{3} \right) - T_{H1} \right) \right] + \left[P_{L2} + \frac{P_{H2} - P_{L2}}{T_{H2} - T_{L2}} \left(\sum_{j=3}^5 \left(\frac{T_{op,j}}{3} \right) - T_{L2} \right) \right] \right\} \quad (1)$$

As the optical radiation entering into the cavity it can be reduced by scattering $S(\lambda)$, window transmittance $T(\lambda)$ and imperfect cavity absorbance $A(\lambda)$. So, the measured optical power P_{op} should be corrected for these parameters [12]. The resultant optical power using Eq. (2) was obtained as 218 μW with an uncertainty at the order of 10^{-4} level.

$$P_{corr.op}(\lambda) = \frac{1}{T(\lambda)} \left[\frac{P_{op}(\lambda)}{A(\lambda)} + S(\lambda) \right] \quad (2)$$

Following the optical power measurements, Ge trap detector was moved to the laser beam path and the generated photocurrent was measured. The

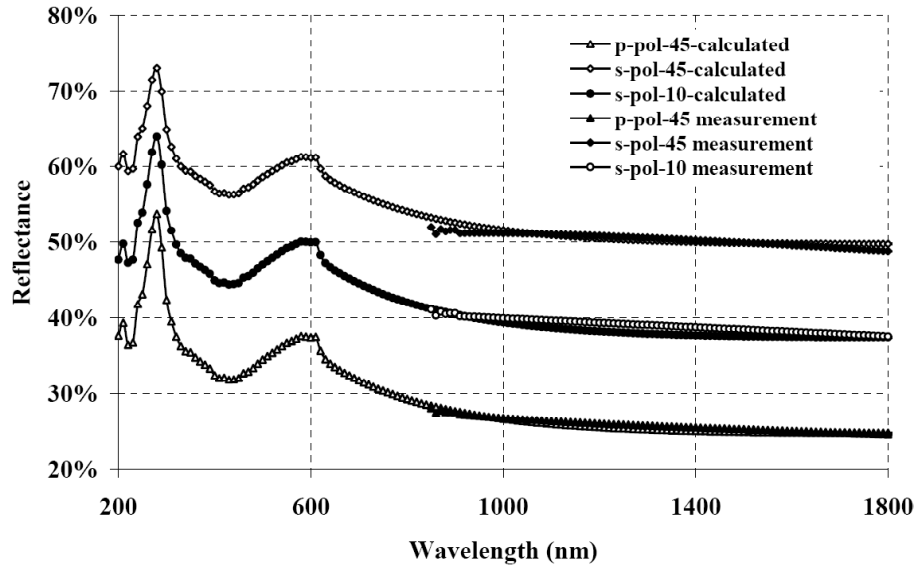


Fig. 3. Measured and calculated reflectance values of Ge photodiode.

ratio of generated photocurrent to incident optical power is called responsivity and using Eq. (3), it can be expressed as [13],

$$R = \frac{V/G}{(P_{corr.op})}, \quad (3)$$

where R is the responsivity, V is the measured voltage and G is the amplifier factor (Volt/Amp.).

The absolute responsivity was obtained with an uncertainty of $\sim 9 \times 10^{-4}$ which besides the partial uncertainties, distributions (normal, rectangular, triangular, etc.) of measurement results and the sensitive coefficients (partial derivatives of each parameters) of the all the parameters in Eqs. (1), (2), and (3), depends also on parameters like change in homogeneity, linearity, polarization dependency of detector, scattering and stability of optical beam, medium temperature, etc.

The responsivity values obtained in this way are limited to the lasers used in the power measurements. To get its behavior in its whole spectral range the responsivity should be expressed as function of wavelength. It is known that as the light beam incident on a photodiode whose output will be affected by the total reflectance and internal quantum deficiency. Hence, the spectral responsivity of a trap detector always expressed as a function of these parameters given as [11],

$$R = [1 - \rho(\lambda)][1 - \delta(\lambda)] \frac{e\lambda}{hc}, \quad (4)$$

where e is the elementary charge, λ is the wavelength in vacuum, h is the Planck constant, c is the speed of light in vacuum, $r(\lambda)$ is the spectral reflectance, $\delta(\lambda)$ is the internal quantum deficiency of trap detector, and $1 - \delta(\lambda)$ is the internal quantum efficiency.

The responsivity values given in Eq. (4) can be calculated via modeling of the reflectance and quantum efficiency parameters.

3.2. Measurements and calculations of reflectance

The reflectance values of Ge photodiode were calculated considering the trap detector geometrical configuration, polarization state of light, angle of incidence of light in this configuration and using the model developed by A. Haapalinnä et al. for the Si photodiodes [14]. Due to the geometry and number of photodiodes present in the trap detector the total reflectance is expressed as

$$\rho_T(\lambda) = \rho(0)\rho_s^2(45)\rho_p^2(45), \quad (5)$$

where the $\rho(0)$, $\rho_s(45)$ and $\rho_p(45)$ are reflections at normal incidence (0°), at 45° with perpendicular (s) and parallel (p) polarizations respectively.

To calculate these reflections, the Fresnel's reflection, transmission equations [14] and optical constants (n , k) of Ge and Si_xN_y were used. The n , k of Ge were calculated by applying Krammer-Kronig dispersion relations to the reflectance of photodiode measured at the angle close to incident angle [15].

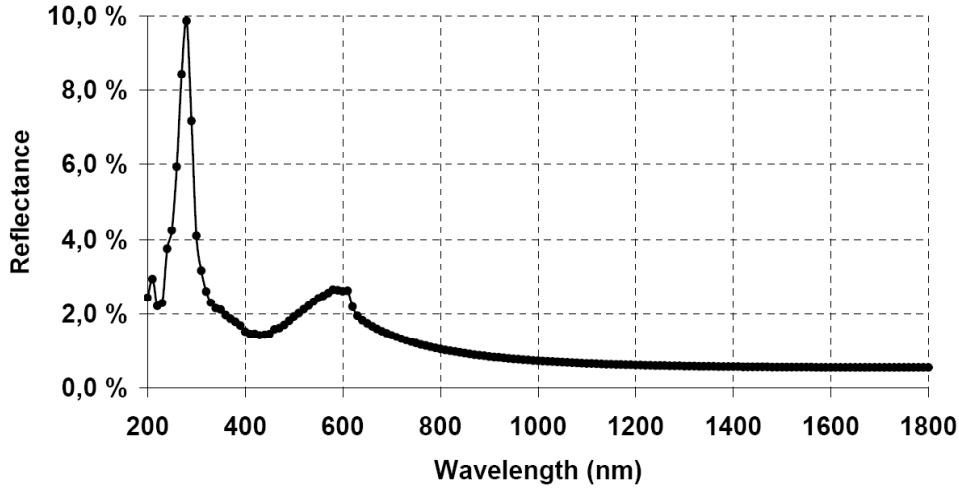


Fig. 4. Calculated reflectance values of Ge photodiode based trap detector.

The surface reflectance's of photodiodes ($\rho(0)$, $\rho_s(45)$, $\rho_p(45)$) within the range from 250 nm to 1650 nm were measured using the measurement system consisting of light source, monochromator, collimator, polarizer, integrating sphere, lock-in amplifier and Si and InGaAs detectors. The reflectance values extrapolated to low wavelengths (from 250 nm to 200 nm) using the relation $\rho(\omega) = \rho(\omega_1) (\omega_1/\omega)$ [16] where ω is the frequency. The refractive index for the antireflective coating was calculated using the relation described by $n(\lambda)_{\text{AR-coating}} = x_1 + x_2/\lambda^2$ [17] where the x_1 and x_2 values are taken as 1.9 and $5.4 \times 10^{-4} \text{ nm}^2$. The calculated reflectance's data were fitted to the measured data by adjusting the anti reflective thickness parameter. The difference between measured and calculated data after the best fit was between 10^{-3} - 10^{-4} level. The anti reflective thickness after the fitting was obtained as 200 nm. Substituting $\rho(0)$, $\rho_s(45)$ and $\rho_p(45)$ into Eq. (4) the reflectance of trap detector were calculated. The result indicates that the reflectance of trap detector is below 1.0% over the wavelengths under the study, this means that in this region the responsivity is insensitive to the reflectance changes, but increases at short wavelengths.

3.3. Quantum Efficiency Calculation

The quantum efficiency (QE) is defined as a degree of effectiveness of the incident radiant flux for producing measurable parameters like temperature, current, etc., in a detector [17]. Depending on the portion of radiant flux that takes part in formation of these effects it can be defined as internal QE and external QE. The internal QE for a photodiode is

the number of electron hole pairs created per absorbed photons; whereas, the external QE is the number of number of electron hole pairs created per incident photons [18].

To calculate the QE of photodiode consider that a flux of photons (F_0) incident on a photodiode, where some portion of that flux undergoes reflection losses, the remaining part transmits through the surface passivating layer, and is absorbed by photodiode, results in generation of electron hole minority carriers. To be able to express the photocurrent in the p-n photodiode drift and diffusion current of carriers given in Eq. (6) should be examined [12,13]

$$J_p = pq\mu_p E - qD_p \frac{dp_n}{dx}, \quad (6a)$$

$$J_n = nq\mu_n E + qD_n \frac{dn_p}{dx}, \quad (6b)$$

where the first terms are drift currents which arise from electric field E at the space charge region, and second terms are diffusion currents due to concentration gradient of carriers, $D_{p,n}$ and $\mu_{p,n}$ are hole (electron) diffusion constant and mobility respectively.

The photon flux inside the photodiode varies exponentially with distance generate electron hole pairs. Some of these carriers undergo recombination and do not contribute to current. Thus, the variation of these carriers inside the photodiode, which is called continuity equation, can be given as [12,13]

$$\begin{aligned} [p(x, t+dt) - p(x, t)] A dx = \\ [F_p(x) - F_p(x+dx)] A dt + (G_p - R_p) A dx dt, \end{aligned} \quad (7a)$$

$$\begin{aligned} [n(x, t+dt) - n(x, t)] A dx = \\ [F_n(x) - F_n(x+dx)] A dt + (G_n - R_n) A dx dt, \end{aligned} \quad (7b)$$

where terms in the left hand side are time rate of change of carriers in $A dx$ volume element, first terms in the right hand side are the change in the photon flux, and G and R are generation and recombination of carriers.

Using the relation between current density and photon flux for electron and holes $J_{n,p} = \pm qF$ and also substituting Eqs. (6a) and (6b) into Eqs. (7a) and (7b) we get the following equations.

$$\frac{\partial p_n}{\partial t} = D_p \frac{\partial^2 p_n}{\partial x^2} - E \mu_p \frac{\partial p_n}{\partial x} + G_p - R_p, \quad (8a)$$

$$\frac{\partial n_p}{\partial t} = D_n \frac{\partial^2 n_p}{\partial x^2} + E \mu_p \frac{\partial n_p}{\partial x} + G_n - R_n. \quad (8b)$$

Since the absorption depth depends on absorption coefficient, we assumed that at short wavelengths negligible amount of photons can be absorbed in the thin p-region. Photons within 850-1650 nm are almost absorbed in the p-region and depletion region, where due to built in field approximately all the generated electron hole pairs contribute to the current and as a result internal QE is assumed to be unity. However, in the n-region due to recombination of carriers the internal QE is expected to deviate much from unity at higher wavelengths. In the light of these assumptions, we calculate internal QE by considering the diffusion current due to minority carriers in n side of photodiode and drift current in the depletion region.

The diffusion current in n side of photodiode may be obtained by considering the electric field in the neutral n region as zero and also by taking into account only steady state condition. Then the first term in the left hand side of Eq. (8a) vanishes and we have

$$D_p \frac{\partial^2 p_n}{\partial x^2} + G - R = 0. \quad (9)$$

Solution of Eq. (9), considering that the electric field is zero in Eq. (8a) gives

$$p_n = p_n(x) \rightarrow I_p = -qAD_p \frac{dp}{dx}, \quad (10)$$

where I_p ($J_p = I/A$) is the minority hole current.

The generation G and recombination R rate parameters in Eq. (9) were defined by considering that the generation rate of electron and hole pairs inside

the photodiode in the both depletion and n regions vary exponentially as a function of absorption coefficient α as $G = (1 - \rho)F_0\alpha e^{-\alpha x}$. Recombination rate in Ge photodiode, which have indirect band gap, is defined by the local energy levels within the band. We used recombination rate defined by Hall, Read, and Shockley and made an assumption that trap energy level is at the mid gap, so for low injection we have [19,20] $R = (p_n - p_{n0})/\tau_p$. The minority carriers in the n side of photodiode can be obtained by solving Eq. (10) and considering the behavior of these carriers at the points $x = W$ (depletion region width) and $x = 0$ (the point too away from the depletion region in the n side). Assuming the behavior of the minority carrier in the mentioned points as $p_n = p_{n0}$ for $x = \infty$, and $p_n = 0$ for $x = W$, their variation as a function of distance obtained as

$$p_n - p_{n0} = [p_{n0} + C e^{-\alpha W}] e^{\left(\frac{W-x}{L_p}\right)} + C e^{-\alpha x} \quad (11)$$

with $L_p = (D_p \tau_p)^{1/2}$ and $C = (1 - \rho)F_0\alpha\tau_p/(1 - \alpha^2 L_p^2)$. Substituting Eq. (11) into Eq. (10) the diffusion current can be obtained as in the following form.

$$I_{diff} = qA(1 - \rho)F_0 \frac{\alpha L_p}{1 + \alpha L_p} e^{-\alpha W} + qAp_{n0} \frac{D_p}{L_p}. \quad (12)$$

The drift current due to field in depletion region can be calculated by integrating all the generated carriers

$$I_{diff} = -qA \int_0^W G(x) dx = qA(1 - \rho)F_0(1 - e^{-\alpha W}). \quad (13)$$

The total current in the examined photodiode is the sum of diffusion and drift current ($I_m = I_{drift} + I_{diff}$). Hence, summing the two expressions given in Eqs. (12) and (13) gives

$$I_m = qA(1 - \rho)F_0 \left(1 - \frac{e^{-\alpha W}}{1 + \alpha L_p}\right) + qAp_{n0} \frac{D_p}{L_p}. \quad (14)$$

This expression is the results of the contribution of number of electron hole pairs (I/q) to the measured current. It is known that inside a photodiode some of the created electron hole pairs due to recombination do not contribute the measured current. So, the total numbers of electron hole pairs created by the absorbed photon should be expressed as $(I_t/q)(1 - \delta)$, where δ is denotes the recombination effects and also called as the quantum deficiency of a photodiode.

Neglecting the leftmost term in Eq. (14), which is due to dark current and is very small, and rewrit-

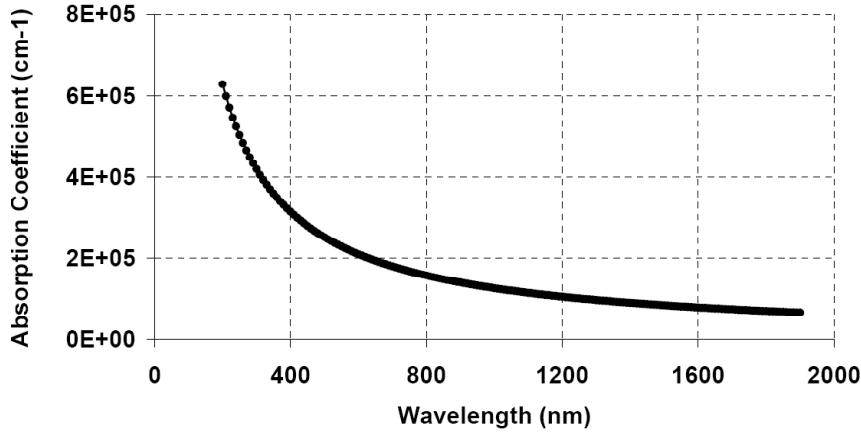


Fig. 5. Absorption coefficient in Ge photodiode as a function of wavelength.

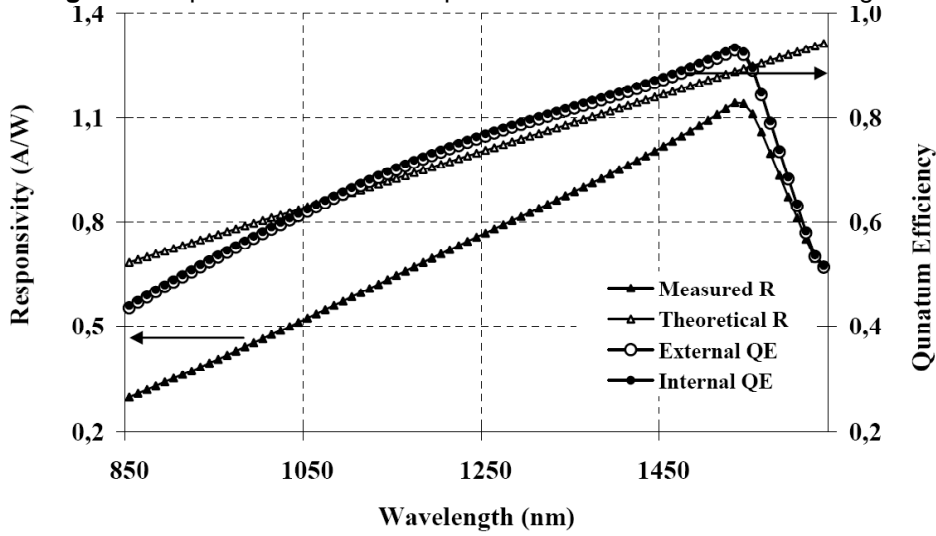


Fig. 6. Quantum efficiency and responsivity of Ge photodiode based trap detector.

ing Eq. (14) in terms of total numbers of electron hole pairs $(I_t/q)(1 - \delta)$ created per incident photons AF_0 we get the relation between external (η_{ext}) and internal QE (η_{int}). Because the term $(I_t/q)/AF_0$ is equal to external QE and $1-d$ is internal QE.

$$\eta_{ext} = \left(\frac{1}{qAF_0} \right)_m = \left(\frac{1}{qAF} \right)_t (1 - \delta) = (1 - \rho) \eta_{int} \left(1 - \frac{e^{-\alpha W}}{1 + \alpha L_p} \right). \quad (15)$$

The unknown parameters in this Eq. (15) are absorption coefficient, depletion layer width and diffusion length. The absorption coefficient can be obtained using the optical constants (n, k) of Ge photodiode and $\alpha = 4\pi k/\lambda$ relation. The calculated absorption coefficient as a function of wavelength is shown in Fig. 5. The other parameters W and L were obtained by fitting the calculated QE values to

measured ones which are calculated using Eq. (4) where the absolute responsivity (R) and reflectance (ρ) values were obtained at the laser wavelengths as described in sections 3.1. and 3.2.

Fig. 6 indicates those internal and external QE of Ge photodiode based trap detectors are close to each other and external QE slightly less than internal QE values. This is expected because from Eq. (15) it can easily be seen that there is a $\eta_{ext} = (1 - \rho)\eta_{int}$ relation between external and internal QE values. This relation also points out how a trap detector removes polarization dependency and reduces reflectance losses of a photodiode. In a single photodiode internal QE is independent of polarization state of incident beam because at different angles of incidence and polarization state, although the absorbed number of photons varies, the ratios of countable events in a photodiode to the absorbed photons are almost the same. External QE on the other hand depends on polarization state of incident beam and

angle of incidence since front layer reflectance depends on polarization state of incident beam.

Having characterizing the reflectance and QE, using Eq. (4) the responsivity of Ge photodiode based trap detector can be determined, Fig. 6.

Ge photodiodes used in the trap detector construction are *p-n* type photodiodes. The *n* and *p* layers are formed by doping Ge with Gallium (Ga) and Arsenic (As) respectively. The front region is coated with Si_xN_y anti reflecting coating. Low responsivity at shorter wavelengths can be related to generations of carriers away from depletion layer that is close to Ge / Si_xN_y interface where recombination are expected to be high. At higher wavelengths, beyond 1550 nm the sharp decrease is considered to be result of direct band gap transitions in Ge [19].

4. CONCLUSION

The construction and realization of the spectral responsivity of Ge based reflection type trap detectors were studied in this work. Different measurement systems were established in order to optically characterize the constructed detector and to calculate its effects on the uncertainty. The scale was linked to high accuracy electrical substitution cryogenic radiometer and was expanded to other wavelengths in its active range by modeling reflectance and QE values.

The usage of the constructed Ge photodiode based trap detector for the determination of responsivity of detectors within its spectral responsivity and linearity range improved the uncertainty about 0.9% in the NIR region compared to previous uncertainty scale which was traceable to Electrically Calibrated Pyroelectric Radiometer. Therefore, the Ge trap detector can be used effectively in metrology especially in the fiber optics communication wavelengths and some other crucial sensors operating at NIR wavelengths.

REFERENCES

- [1] T.J. Quinn and J.E. Martin // *Metrologia* **128** (1999) 155.
- [2] E. Zalewski and C.R. Duda // *Applied Optics* **22** (1983) 2867.
- [3] N.P. Fox // *Metrologia* **28** (1991) 197.
- [4] K.D. Stock, R. Heine and H. Hofer // *Metrologia* **40** (2003) 163.
- [5] A. Lamminpaa, M. Noorma, T. Hyyppa, F. Manoocheri, P. Karha and E. Ikonen // *Meas. Sci. Technol.* **17** (2006) 908.
- [6] J.M. Palmer // *Metrologia* **30** (1993) 327.
- [7] T. Kùbarsepp, P. Kàrhà and E. Ikonen // *Applied Optics* **36** (1997) 2807.
- [8] J.H. Lehman and C.L. Cromer // *Applied Optics* **41** (2002) 6531.
- [9] H.J. Mùller, *Semiconductors for Solar Cells* (John Wiley and Sons. Inc., New York, 1993).
- [10] B.G. Streetman, *Solid State Electronic Devices, 4th ed.* (Prentice Hall Series in Solid State Physical Electronics, 1995).
- [11] K.M. Nield, J.F. Clare, J.D. Hamlin and A. Bittar // *Metrologia* **35** (1998) 581.
- [12] T.R. Gentile, J.M. Houston, J.E. Hardis, C.L. Cromer and A.C. Parr // *Applied Optics* **35** (1996) 1056.
- [13] E.F. Zalewski and J. Geist // *Applied Optics* **19** (1980) 1214.
- [14] A. Haapalinna, P. Karha and E. Ikonen // *Applied Optics* **37** (1998) 729.
- [15] M.A. Gren // *Solar Energy Materials & Solar Cells* **92** (2008) 1305.
- [16] D.L. Greenaway and G. Harbeke, *Optical Properties and Band Structure of Semiconductors* (Pergamon Press, Oxford, 1968).
- [17] Marco Antonio López-Ordoñez, Optical characterization of Ge- and InGaAs semiconductor detectors for high accuracy optical radiant power measurements in the near infrared, (Ph. D Thesis, Technische Universität Carolo-Wilhelmina zu Braunschweig, 2008).
- [18] E.F. Zalewski and C.C. Hoyt // *Metrologia* **28** (1991) 203.
- [19] K.D. Stock, In: *New Developments and Applications in Optical Radiometry*, ed. N. P. Fox and D. H. Nettleton (Inst. Phys. Conf. Ser. No 92, Bristol: IOPP, 1989), p. 59.
- [20] S.M. Sze, *The Physics of Semiconductor Devices* (Wiley, New York, 1969).